

Nano- and micro-scale resolution in ancient obsidian artefact surfaces: The impact of AFM on the obsidian hydration dating by SIMS-SS

I. Liritzis^{*1}, N. Laskaris^{**1}, and M. Bonini²

¹ Laboratory of Archaeometry, Dept. of Mediterranean Studies, University of the Aegean, 1 Demokratias Ave, Rhodes 85100, Greece

² CSGI, Dept of Chemistry, Room #18, via della Lastruccia 3, 50019 Sesto Fiorentino (FI), Italy

Received 27 November 2007, revised 11 June 2008, accepted 16 June 2008

Published online 18 September 2008

PACS 68.35.Ct, 68.37.Ps, 82.80.Ms

* Corresponding author: e-mail liritzis@rhodes.aegean.gr, Phone: +302241099385, Fax: +302241099320

** e-mail n.laskaris@ieee.org, Phone: +306947026891, Fax: +302241099320

The prehistoric tools made by natural glass of obsidian can be dated by the recent method of the secondary ion mass spectrometry with the surface saturation using the surface saturation approach (SIMS-SS). In its initial tests, the method inherited some limitations mainly derived from surface roughness. Indeed, the surface irregularities i.e. presence of wells,

cracks, pits, crystals and/or crests, induce uncertain errors in the dating procedure. Here, we provide further images of the Atomic Force Microscopy (AFM) of obsidian surfaces and discuss the impact of AFM results on the SIMS-SS dating, investigating the problematic non-smoothed surfaces.

© 2008 WILEY-VCH Verlag GmbH & Co. KGaA, Weinheim

1 Introduction

1.1 SIMS measurements and profile

SIMS and AFM analyses were applied on nine prehistoric obsidian artifacts. SIMS were conducted at the commercial laboratory of Evans East, East Windsor, NJ, the profiles were collected using PHI model 6300 and 6600 quadrupole-based secondary ion mass spectrometers. A 5 keV Cs⁺ primary ion beam with an impact angle of 60° with respect to surface normal was used and negative secondary ions were detected. The measurements were performed using a 300x300 micron ion beam raster. The depth scale accuracy by SIMS for archaeological samples is within 5-10%. This translates into an estimated error of ±0.05 μm. This value is not equivalent to the ±0.01-0.03 μm standard deviation usually associated with SIMS because of the irregular surface topography present on naturally cleaved samples.

Even if SIMS is amongst the high precision, non-optical, depth profiling techniques for measuring the width of the hydration rim, depth resolution is limited by atomic mixing effects, the flatness of the analyzed area. Also the dynamic range of depth profiles is limited by crater edge effects, neutral beam effects and several types of instrumental background [1]. Irregular and/or inhomogeneous

surfaces cause problematic diffused regions and, therefore, produce uncertain ages. According to our model, H₂O molecules choose various diffusion paths in a non-homogeneous way, as the size-dependent mechanism [2] assumes that water molecules of radius $r_w = 0.15 \mu\text{m}$ occupy interstitial sites of the obsidian and pass through “doorways” of radius r_D jumping from one doorway to another [2]. The $r_D = 0.1 \mu\text{m}$ derives from equation regarding activation energy E , which is recognized as the elastic energy to dilate a spherical cavity from radius r_D to r . Therefore, cavities, holes and troughs of surface topological anomalies will have an impact by distorting initial SIMS profiles which includes the SS layer. In the emerged pattern for safe location of SS, there are cases where the location of SS and/or the polynomial fitting are both problematic. The uncertain ages are linked to the surface topography. An approach to such problems is the use of Atomic Force Microscopy (AFM). AFM is a well-suited technique in the roughness analysis of obsidian surfaces [3, 4]. An indication of the linear correlation between SIMS diffused profile properties and surface roughness measured by AFM reconfirms their interdependence. This aids selection of appropriate obsidian samples/surfaces for dating. It is in-

interesting to note that samples which were macroscopically the less homogeneous, is among the group of the more often encountered ones, and such macroscopic irregularities are avoided. AFM images are very important data for proper choice of the spot where SIMS analysis is performed, which in certain cases is not easy to locate. They represent a crucial step in the reliability of the obtained ages. When this condition is properly fulfilled, the accuracy the results and suitability of the samples should directly depend on the roughness of the sample.

1.2 SIMS-SS dating method The SIMS-SS dating method is based on the modeling of the H_2O concentration versus depth profiles which follows Fick's law of diffusion and the use of saturation surface approach. According to this new method the age equation depends on the H^+ concentration (C_s) in the saturation layer near to the surface, the hydration depth of this layer (X_s), the connate or internal concentration of water (C_i), the diffusion coefficient (D) and polynomial coefficients derived from the 3rd order polynomial fitting of Sigmoid curve [2, 5, 6]. The dating results compared with radiocarbon ages reveal a convergence that reinforces the new dating approach. The produced age equation has been supported by dated world examples for more than 40 obsidians with age ranging from 600 to 30,000 years B.P.

The determination of the SS layer is made along two ways. The first procedure is the repeated derivatives approach starting from the initial points and covering the whole diffused region, and the second procedure is the sliding progressive regressions to determine a near zero slope. These two procedures result to a high precision method for the location of the SS layer; however the latter has shown cases where the location of SS is problematic which is linked to the surface topography.

Here we investigate AFM 2D and 3D images from prehistoric obsidian tools from Aegean area (Islands of Yali, Youra, Mykonos and Sarakinos cave at central Greece) and Asia Minor, NW Turkey, and correlate the roughness results with the SIMS profile of the same obsidian tool. We have already shown elsewhere a first approach to this correlation [7], but here we present a more detailed analysis of the diffused region of the SIMS profile with the roughness and also with the SS layer's attributes.

1.3 AFM measurements An Explorer TMX 2000 microscope (Topometrix) was employed for the imaging of our obsidian tools with AFM using a $100 \times 100 \mu m$ xy, $10 \mu m$ z air scanner and a silicon "V" shaped cantilever with an integrated pyramidal tip for contact imaging. The images were taken at room temperature in contact mode and they were processed by flattening in order to remove the background slope. The scanner used to perform the measurements has a maximum z excursion of $10 \mu m$, corresponding to the maximum difference in the height scale of the sample that could be accessed with our instrument

(gaps bigger than $10 \mu m$ cannot be imaged by our instrument).

The surface topographic details observed in the nano- and micro-scale (Figs. 1 and 2) could not be detected using Polarized Light Microscope or Scanning Electron Microscope. These features are cracks and voids, which were sometimes within the first $10 \mu m$ of the tool surface and a range in depth of some 100 nm . These cracks and voids probably make the SIMS measurement problematic and therefore any age result has high uncertainty.

However there are some areas free of voids and cracks and with small surface roughness which are ideal for SIMS and therefore to produce an age result with high accuracy.

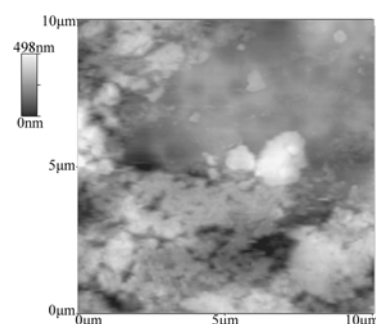


Figure 1 a) 2D AFM image for sample Fikirtepe-7 (Asia Minor).

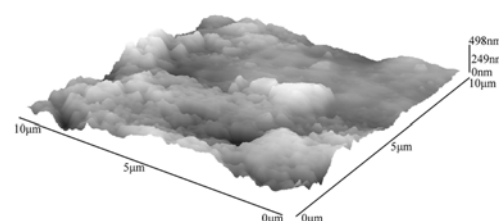


Figure 1 b) 3D AFM image for sample Fikirtepe-7 (Asia Minor).

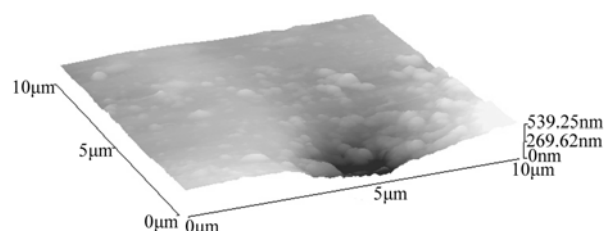
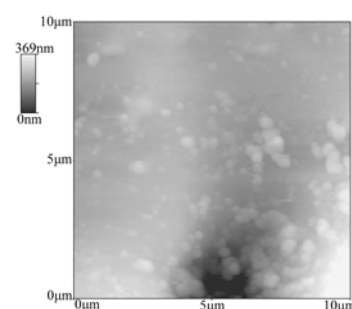


Figure 2 a), b) 2D and 3D AFM images for sample Ulucak (Asia Minor).

2 Results and discussion on the obsidian surface analysis by AFM

2.1 Obsidian surface analysis by AFM The first step in our investigation for a correlation between the surface anomalies of the obsidian tool and the SIMS profile is to calculate a roughness parameter. Table 1 shows the list of samples investigated with AFM and the roughness parameter R_a which is the arithmetical mean deviation of the surface profile and indicates the amount of irregular features of the surface. Figure 3 shows a histogram of this parameter.

Table 1 The roughness parameter R_a . GR is for samples from Greece and AM for samples from Asia Minor, Turkey.

Sample	R_a [nm]
MYC-1 (GR)	27.66
ULUCAK (RHO-20-3) (AM)	36.56
YAL-1 (GR)	13.47
DL-90-282 (AM)	4.08
TURK-6 (AM)	7.11
SAR-2 (GR)	27.63
FIKIRTEPE-7 (AM)	62.89
YR-3 (GR)	6.78
MYC-7 (GR)	25.67

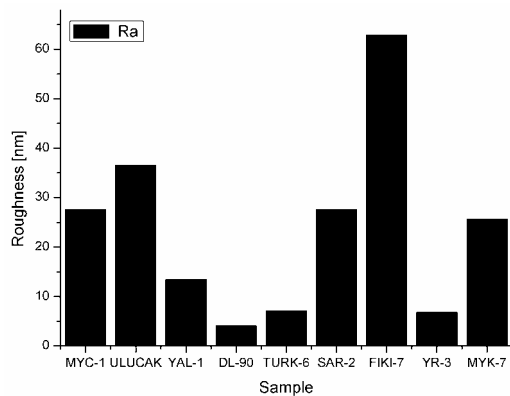


Figure 3 Histogram representation of R_a .

The group of samples that is fairly safe to apply the dating method includes samples YAL-1, DL-90, TURK-6, YR-3. In the case of non datable samples or samples with high uncertainty are namely samples with high surface roughness like FIKIRTEPE-7 and ULUCAK.

Elsewhere [7] we have already correlated the roughness parameter R_a with the R_{std} factor. R_{std} is the standard deviation of the residuals of the diffused region points with its linear fitting. In other words, the linear regression fit ($y = a+bx$) of the diffused region (see region 1 in Fig. 4) is calculated, and then the residuals of this line is used with the respectively SIMS points to calculate the standard deviation.

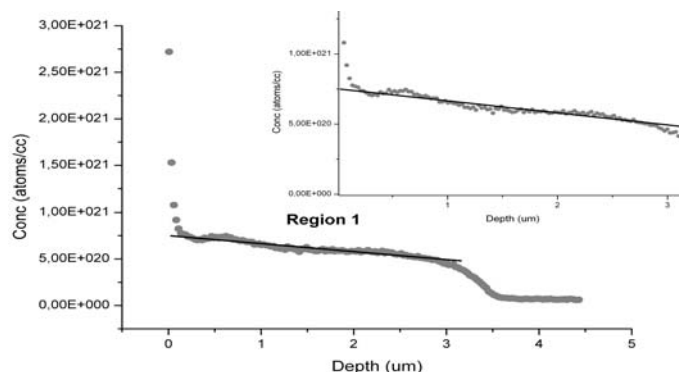


Figure 4 A SIMS profile of water concentration versus depth and the linear fit in the diffused region for sample YR-3 (Youra Island, Greece).

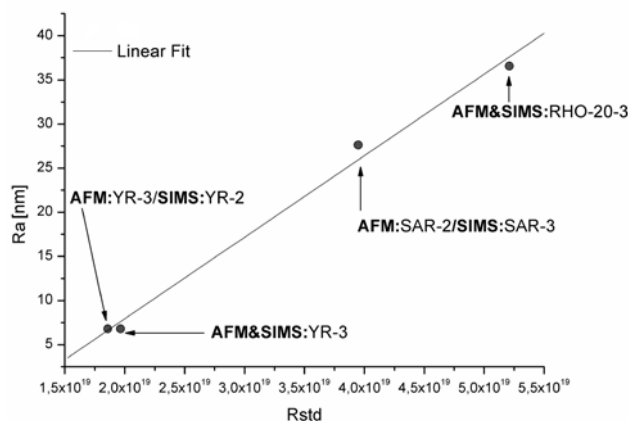


Figure 5 The R_a factor plotted in relation with R_{std} .

This correlation reveals a linear relationship between the parameter R_a and the spread of points in the diffused area (Fig. 5), which support the assumption that rough surfaces affect the dispersion of the SIMS points and therefore the age calculation and the accuracy of the result.

2.2 Further calculations in the AFM-SIMS correlation In order to have a clearer view in the linear correlation of the surface roughness (represented by the R_a factor) with the dispersion of SIMS points and therefore with the accuracy of the age calculation we tried to correlate the surface roughness with the standard deviation (\pm error) of the saturation concentration (C_s).

In Table 2 the surface saturation layer attributes for four samples are shown, were the concentration error is in gmol/cc but the correlation with the R_a is in atoms/cc . This is because age calculations are in gmol/cc but for a clearer view of dispersion of atoms of water we use atoms/cc .

This standard deviation of saturation concentration (\pm error in atoms/cc) $C_{s\text{ std}}$ is correlated with AFM factor R_a , based on the rationale that the smoother the surface the lesser dispersion and smoother the SIMS diffusion profile.

Table 2 Data of saturation layer for the samples, C_{sur} is the concentration and X_{sur} is the depth of the Saturation Layer.

Sample	C_{sur} (gmol/cc)	X_{sur} (cm)
Ulucak (RHO-20-3)	0.001814 $\pm 3.36\text{e-}5$	0.0001764 $\pm 3.19\text{e-}6$
SAR-4	0.0009746 $\pm 1.53\text{e-}5$	0.0001283 $\pm 3.6\text{e-}6$
YR-2	0.0007930 $\pm 1.30\text{e-}5$	2.612e-5 $\pm 2.19\text{e-}6$
YR-3	0.0005165 $\pm 8.69\text{e-}6$	0.00011835 $\pm 4.04\text{e-}6$

part of % change of saturation concentration is plotted against the age of a sample.

3 Conclusion The Nano- and Micro- scale resolution of ancient obsidian artifact surfaces is well investigated by AFM. This has an impact on the obsidian hydration dating by SIMS-SS. A linear correlation between the roughness parameter derived from AFM measurements with the standard deviation of the points in the diffused region of a SIMS profile. Moreover, an age dependence on concentration changes is observed, the more irregular a surface is, the more uncertain is the age. AFM technique is capable for a vital pre-SIMS examination of the artifact surface to decide the appropriate low roughness surface for SIMS measurements

References

- [1] C. W. Magee and R. Honing, *Surf. Interface Anal.* **4**(2), 35 (1982).
- [2] I. Liritzis, *Archaeometry* **48**(3), 533 (2006).
- [3] J. G. Simpson et al., *Langmuir* **15**, 1429 (1999).
- [4] J. D. Kiely and A. D. Bonnell, *J. Vac. Sci. Techn. B* **15**, 1483 (1997), and topometrix SPMlab software version 3.05.
- [5] I. Liritzis et al., *J. Radioanal. Nucl. Chem.* **261**(1), 51 (2004).
- [6] I. Liritzis and T. Ganetsos. *Appl. Surf. Sci.* **252**(19), 7144 (2006).
- [7] I. Liritzis, M. Bonini, and N. Laskaris, *Surf. Interface Anal.* **40**, 458 (2008).

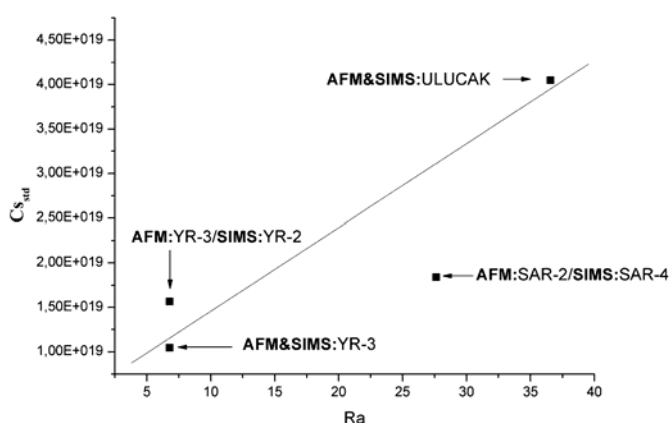


Figure 6 The standard deviation of the saturation concentration $C_{s \text{ std}}$ plotted against R_a .

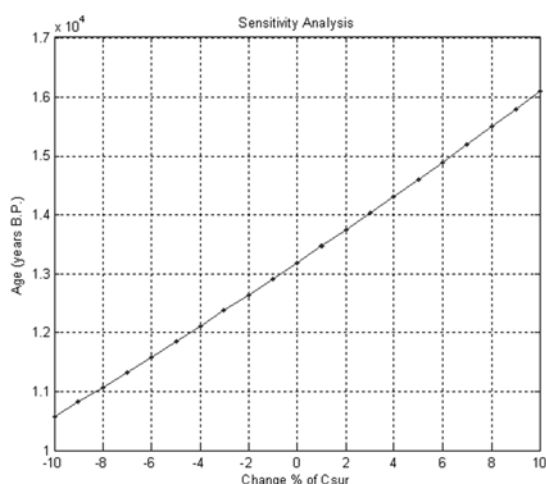


Figure 7 Age variation per % change of saturation concentration for sample YR-3 (Yours Island, Greece).

For a clearer view, Fig. 6 gives the plot of the standard deviation of saturation concentration against the R_a factor. Here it is notable the linear correlation between the standard deviation and the roughness. Finally in Fig. 7 the im-